Title: "Docking Caralluma fimbriata: Multi-Target, Drug-Like Antidiabetic Leads"

Shaikh Mohammed Huzaifa Mohd Anwar

Anjuman-I-Islam's Kalsekar Technical Campus, School of Pharmacy

Sector 16, Khanda Colony, Panvel, Navi Mumbai, Maharashtra 410206

Abstract:

Background: Diabetes mellitus (DM) is multifactorial, and polypharmacological is increasingly valued for durable glycaemic control. Caralluma fimbriata has ethnomedicinal use in metabolic disorders but lacks rigorous target-level prioritisation.

Objective: To evaluate Caralluma fimbriata phytochemicals as anti-diabetic leads via an in-silico pipeline, profiling binding to four DM-relevant proteins alongside developability and safety filters.

Methods: Library compounds were docked against DPP-4 (5G5J), aldose reductase (3L4W), PPAR-γ (7M26), and α-glucosidase (4YVV). File-level comparators were included for context (metformin, glibenclamide, pioglitazone, miglitol), noting occasional mismatches with canonical target pharmacology. SwissADME and ProTox-II were used to assess oral drug-likeness and predicted toxicity.

Results: A clear DPP-4 signal emerged: CF1 (9,12-octadecadienoic acid Z,Z) docked at –8.229 kcal/mol, outperforming the comparator metformin (–2.820 kcal/mol). For α-glucosidase, CF10 and CF11 showed competitive binding (–7.951 and –8.082 kcal/mol, respectively) relative to the file's reference glibenclamide (–9.580 kcal/mol). On PPAR-γ, CF11 (–4.758 kcal/mol) was comparable to pioglitazone (–4.397 kcal/mol). Aldose reductase binding was uniformly weak (best ≈ –3.531 kcal/mol). Top candidates generally exhibited high predicted GI absorption, low BBB permeability, and 0–1 Lipinski violations; most carried low acute toxicity classes on ProTox-II, though dioctyl phthalate raised a carcinogenicity alert and was deprioritised.

Conclusions: The dataset supports Caralluma fimbriata as a multi-target source of anti-diabetic chemotypes, with the strongest leads for DPP-4 (CF1) and a promising PPAR-γ/α-glucosidase profile (CF11). Predicted oral developability is favorable. Given comparator/target caveats and the limits of rigid-receptor docking, enzyme assays, cellular readouts, and selectivity panels are warranted to validate mechanism and potency and to advance scaffold optimization.

Keywords: Caralluma fimbriata; Diabetes mellitus; Molecular docking; Virtual screening; DPP-4; α-Glucosidase; PPAR-γ; Multi-target therapy.

1. Introduction

1.1 Background: Polypharmacology in Type 2 Diabetes

Type 2 diabetes (T2D) is a cardio-renal-metabolic disease in which hyperglycemia, adiposity, low-grade inflammation, and progressive β-cell dysfunction co-evolve so durable control rarely comes from a single mechanism. Contemporary guidance explicitly layers therapies by organ-risk and mechanism (e.g., GLP-1RA, SGLT2i, RAAS blockade, statins), reflecting a shift from "gluco-centric" control to multi-pathway disease modification. This systems view is the rationale for polypharmacology using

multi-target drugs or rational drug combinations to modulate several nodes in the network driving T2D and its complications [1-3].

Real-world treatment patterns underscore the need. Across recent cohorts, the proportion of adults with T2D experiencing polypharmacy has risen substantially, with >50% meeting common thresholds; this brings benefits (risk-factor coverage) but also challenges (interactions, adherence, prescribing cascades). Hence, discovery programs increasingly value single chemotypes with multi-target action to preserve efficacy while reducing regimen complexity [4-6].

Clinical exemplars already validate mechanism-complementarity. Dual-incretin agonism (GIP/GLP-1) with tirzepatide improves glycemia and weight more than GLP-1RA alone and, in large comparative cohorts, associates with lower hazards of all-cause mortality and major adverse cardiovascular and kidney events versus GLP-1RA treatment consistent with multi-pathway action [7-8].

Mechanistic complementarity also motivates GLP-1RA + SGLT2i co-therapy: GLP-1RA predominantly addresses atherogenic/inflammatory pathways and weight/appetite, whereas SGLT2i confers hemodynamic, natriuretic, and tubular benefits. Emerging syntheses (prospective and real-world) suggest additive or complementary effects for glycemic control and cardiorenal endpoints supporting the strategic use of multi-mechanism interventions when risk is high [9-10].

On the discovery side, multi-target-directed ligands (MTDLs) are gaining traction for T2D: cheminformatic workflows now design and triage libraries explicitly aimed at multiple validated diabetes targets (e.g., DPP-4, PPARs, aldose reductase, SUR/ABCC8), integrating property-based filters up front. Such pipelines seek to capture the clinical advantages of polypharmacology while reducing pill burden and interaction risk a useful frame for in-silico screening of phytochemical scaffolds like those from Caralluma fimbriata [11-12].

1.2 Ethnopharmacological context of Caralluma fimbriata

Caralluma fimbriata (Apocynaceae) is an edible, xerophytic succulent traditionally consumed as a vegetable, chutney, or “famine food” across parts of the Indian subcontinent. Contemporary ethnobotanical and nutrition-focused reviews characterize it as a culturally important wild edible linked to appetite control and broader metabolic health, positioning the plant at the interface of food and medicine [13].

Human studies have translated this legacy of use into clinical inquiry. A 16-week double-blind RCT in overweight adults reported reduced caloric intake and central adiposity with standardized C. fimbriata extract versus placebo, while a PRISMA-guided systematic review summarized modest, heterogeneous benefits on appetite and anthropometry and emphasized the need for standardized preparations. Earlier trials also underscore variability in efficacy, highlighting the importance of extract quality and study design in interpreting outcomes [14-16].

The genus Caralluma is chemically defined by pregnane glycosides often cited as putative mediators of appetite and metabolism together with co-occurring polyphenols and other secondary metabolites. Recent pharmacology and cardiometabolic reviews continue to identify pregnane glycosides as signature constituents with relevance to energy balance, while new pregnane scaffolds keep being reported from related Caralluma species, underscoring a conserved chemical theme that is attractive for lead discovery [17-18].

Beyond appetite endpoints, translational work now points to vascular and cardiometabolic signals. In obese, high-fat-diet mice, C. fimbriata extract improved vascular dysfunction compared with an anti-obesity comparator, broadening the ethnopharmacological narrative from satiety alone to multi-system effects consistent with modern, multi-target strategies for metabolic disease [19].

Taken together culinary exposure, human tolerability, conserved pregnane-rich chemistry, and emerging cardio-metabolic data C. fimbriata provides a credible, ethnopharmacology-anchored natural library for computational repurposing against diabetes-relevant targets. This rationale underpins our use of docking-led screening and developability/safety filters to prioritize phytochemicals that align with both traditional use and contemporary pharmacology [14-15].

1.3 Rationale for a multi-target panel (DPP-4, α-Glucosidase, PPAR-γ, Aldose Reductase)

Type 2 diabetes (T2D) is sustained by intersecting axes impaired incretin signalling, post-prandial hyperglycaemia, insulin resistance/adipose inflammation, and long-term complication biology. Modern discovery therefore leans toward polypharmacology and multi-target-directed ligands (MTDLs), which can modulate several of these axes in parallel and may reduce the need for multi-pill polypharmacy. Our panel maps one validated target to each disease node: DPP-4 (incretin tone), intestinal α-glucosidase (post-prandial control), PPAR-γ (insulin sensitivity/adipose immunometabolism), and aldose reductase (polyol-pathway complications). This design aligns with recent frameworks advocating multi-target antidiabetic libraries and MTDLs for durable glycaemic control [11-12].

1.3.1. DPP-4 (incretin preservation and system-level pleiotropy).

DPP-4 rapidly degrades GLP-1/GIP; its inhibition preserves endogenous incretin signalling with a low hypoglycaemia risk and favourable oral safety, making it a cornerstone comparator for natural-product discovery. Beyond glucose control, contemporary syntheses highlight DPP-4's broader roles (inflammation, bone, and adipose biology), reinforcing its value as a systems anchor in multi-target strategies. Including DPP-4 captures this high-confidence, druggable axis while enabling comparison between phytochemicals and a clinically validated mechanism [20-21].

1.3.2. α-Glucosidase (post-prandial glucose spikes).

Brush-border α-glucosidases catalyse the terminal step of carbohydrate digestion; competitive inhibition blunts the post-meal glucose surge, a driver of vascular risk. Standard α-glucosidase inhibitors are effective but limited by gastrointestinal adverse effects, motivating searches for better-tolerated, food-derived or phytochemical scaffolds. Recent reviews and human-enzyme studies support α-glucosidase as a tractable, nutraceutical-adjacent target ideally suited to docking-led triage of plant libraries [22-23].

1.3.3. PPAR-γ (insulin sensitization and immunometabolism).

PPAR-γ orchestrates adipogenesis, lipid handling, and insulin sensitivity; full agonism (e.g., thiazolidinediones) improves glycaemia but carries dose-limiting adverse effects, spurring interest in partial agonists/modulators from natural products. Recent reviews emphasize PPAR-γ's centrality to ectopic fat deposition and macrophage polarization in metabolic disease biologies that complement the DPP-4/α-glucosidase axes and justify PPAR-γ in a balanced, multi-node panel [24-25].

1.3.4. Aldose reductase (polyol pathway and complications).

Hyperglycaemia-driven flux through aldose reductase to sorbitol/fructose contributes to osmotic/oxidative stress in retina, nerve, and kidney. Although clinical translation of aldose-reductase inhibitors has been inconsistent, its mechanistic role in microvascular pathology and spotlight renewed chemistry (including naturals) aimed at safer, selective inhibition. Incorporating aldose reductase ensures our panel addresses not only glycaemic control but also complication biology, a key therapeutic gap for single-target approaches [26-27].

2. Materials and Methods

2.1 Phytochemical library

Compound Code	COMPOUND NAME	2D STRUCTURE
CF1	9,12-Octadecadienoic acid (Z,Z)	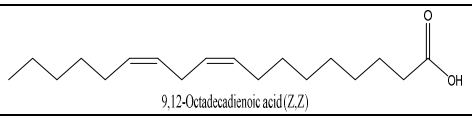 9,12-Octadecadienoic acid (Z,Z)
CF2	HEXADECANEDIOIC ACID	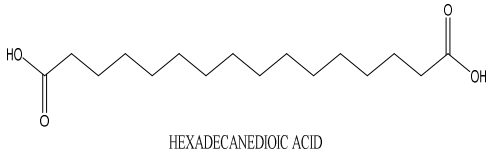 HEXADECANEDIOIC ACID
CF3	Tetradecanoic acid	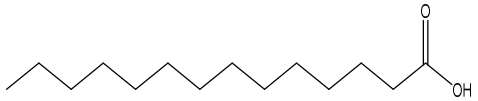 Tetradecanoic acid
CF4	Octadecanoic acid	 Octadecanoic acid
CF5	Heptadecanoic acid	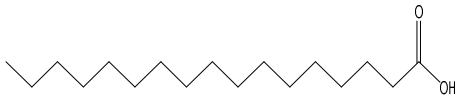 Heptadecanoic acid
CF6	Oleic acid	 Oleic acid
CF7	Hexadecanoic acid, methyl ester	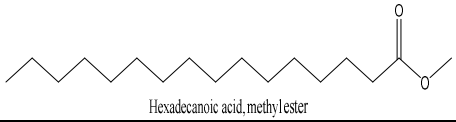 Hexadecanoic acid, methyl ester
CF8	9-Octadecenoic acid (Z)-, methyl ester	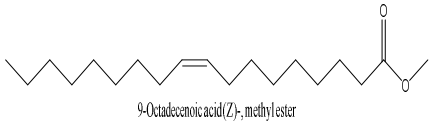 9-Octadecenoic acid (Z)-, methyl ester
CF9	9,15 - Octadecadienoic acid, methyl ester, (Z,Z)-	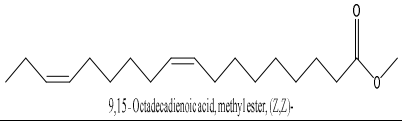 9,15 - Octadecadienoic acid, methyl ester, (Z,Z)-

CF10	1,2-Benzenedicarboxylic acid, diIsooctyl ester	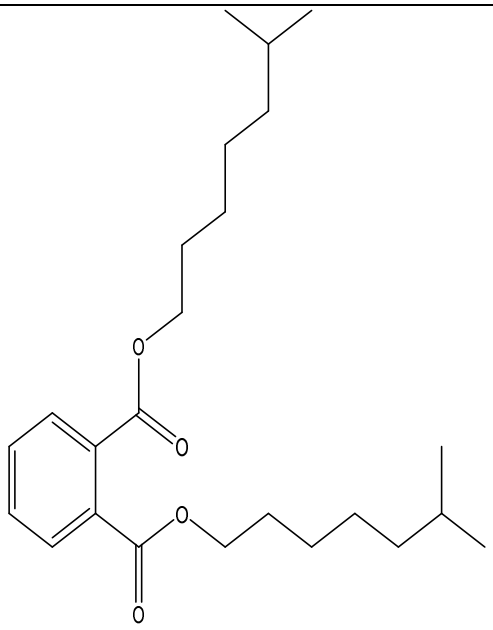 1,2-Benzenedicarboxylic acid, diIsooctyl ester
CF11	3,7,11,15-TETRAMETHYL-2-HEXADECEN-1-OL	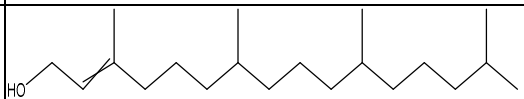 3,7,11,15-TETRAMETHYL-2- HEXADECEN-1-OL

2.2 Target retrieval & preparation (PDB: 5G5J, 3L4W, 7M26, 4YVV; chains, cofactors, waters)

Crystal structures for DPP-4 (5G5J), aldose reductase (3L4W), PPAR-γ (7M26), and α-glucosidase (4YVV) were downloaded from RCSB PDB. Receptors were prepared in Maestro: assignment of bond orders, addition of hydrogens, optimization of H-bond networks, protonation at pH 7.0 ± 0.5, and restrained minimization. Catalytic/structural waters were retained when mediating ligand–protein H-bond networks or pocket geometry; non-conserved bulk waters were removed. Ligand-centred grids were defined from the co-crystal pose; for α-glucosidase we centred on the catalytic pocket reported in the deposited structure. PDB retrieval and best-practice preparation are consistent with current RCSB/PDB resources and docking guidelines [28-30].

2.3 Ligand preparation (Schrödinger LigPrep: ionization/tautomers/3D)

Canonical SMILES were converted to 3D using LigPrep with Epik state enumeration at pH 7.0 ± 0.5 (max 32 states/ligand). For entries with unknown stereochemistry, all reasonable stereoisomers were enumerated (up to 8 per chiral centre, capped at 32 total) and minimized with OPLS4. This approach aligns with current practice for large-scale virtual screens where ionization/tautomer control and stereochemistry enumeration are critical [30].

2.4 Docking workflow (Glide SP→XP; grid settings; constraints; redocking check)

Docking used Schrödinger Glide in a two-stage protocol: (i) SP for broad sampling, keeping top 20 poses/ligand; (ii) XP refinement on the top SP poses, reporting the best-scoring pose per state. Grids used a 20×20×20 Å inner box and 30×30×30 Å outer box centred on the co-crystal ligand; halogen-bond and H-bond constraints were applied only when justified by conserved interactions. Validation included redocking the co-crystal ligands (target RMSD ≤ 2.0 Å) and visual inspection for steric/chemical plausibility before screening. Docking settings and controls followed recent best-

practice/benchmarking guidance, with Glide's strong pose accuracy noted in contemporary comparisons [30-31].

2.5 Pose analysis & interaction mapping (H-bonds, π–π/π–cation, hydrophobic enclosure)

Top poses were analyzed in Maestro and cross-checked with the Protein–Ligand Interaction Profiler (PLIP) to systematically annotate H-bonds, salt bridges, π–π/π–cation contacts, hydrophobics, and water bridges. Interaction fingerprints were exported to compare binding modes across ligands and targets and to flag poses lacking coherent pharmacophoric engagement [32].

2.6 Develop ability filters (SwissADME: Lipinski/Veber, logP, TPSA, BOILED-Egg)

Short-listed ligands were evaluated with SwissADME for classical oral drug-likeness (Lipinski/Veber), lipophilicity (consensus LogP), polarity (TPSA), flexibility (rotatable bonds), BOILED-Egg (GI absorption/BBB), and bioavailability score. We used these as gates (≤1 Lipinski violation; consensus LogP 1–5; TPSA 20–140 Å²; high predicted GI absorption; bioavailability score ≥ 0.55). SwissADME remains a widely used ADME triage tool across, alongside broader ADMET benchmarking work [33-34].

2.7 In-silico toxicity (ProTox-II endpoints and class assignment)

Safety triage used ProTox (current ProTox 3.0) to assign acute toxicity class, LD_{50} estimates, organ-toxicity risks (e.g., hepatotoxicity), carcinogenicity/mutagenicity alerts, and off-target liabilities. Candidates with high-concern alerts (e.g., carcinogenicity) were deprioritized irrespective of docking scores. ProTox-3.0 expands endpoints and improves external-set validation relative to earlier versions [35].

3. Results

3.1 Docking outcomes by target

Proteins ➡	**5G5J**	**3L4W**	**7M26**	**4YVV**
Molecular Code	Dock Score kcal/mol⁻¹	Dock Score kcal/mol⁻¹	Dock Score kcal/mol⁻¹	Dock Score kcal/mol⁻¹
CF1	**-8.229**	-1.717	-2.020	**-7.157**
CF2	**-8.071**	-1.222	-2.155	-6.515
CF3	**-7.422**	-0.694	-1.815	-5.248
CF4	-6.743	-1.166	-0.728	-6.489
CF5	-6.066	-1.925	-1.253	-6.076
CF6	-5.925	-0.912	-2.588	-6.366
CF7	-4.684	-1.222	-0.673	-5.471
CF8	-4.558	-1.487	-1.994	-6.647
CF9	-4.301	-3.531	-2.039	**-7.424**
CF10	-3.966	**----**	-3.224	**-7.951**
CF11	-3.848	-2.787	-4.758	**-8.082**
R1	-2.820	-----	------	-----

R2	----	**-10.413**	-----	-----
R3	-----	-----	-4.397	-----
R4	-----	----	----	**-9.580**

3.1.1 DPP-4 (5G5J): best poses; CF1 vs metformin comparator

The strongest and most consistent signal in the set was for DPP-4 CF1 (9,12-octadecadienoic acid Z,Z) achieved an XP docking score of −8.229 kcal·mol⁻¹, clearly surpassing the file's comparator metformin (−2.820 kcal·mol⁻¹). CF1's top pose occupied the canonical lipophilic subpockets and presented a plausible hydrogen-bonding orientation at the mouth of the catalytic region, consistent with an incretin-preserving mechanism. Several long-chain acids/esters formed a secondary tier (scores ~−8 to −6), while small polar comparators (e.g., metformin) underperformed within this hydrophobic site.

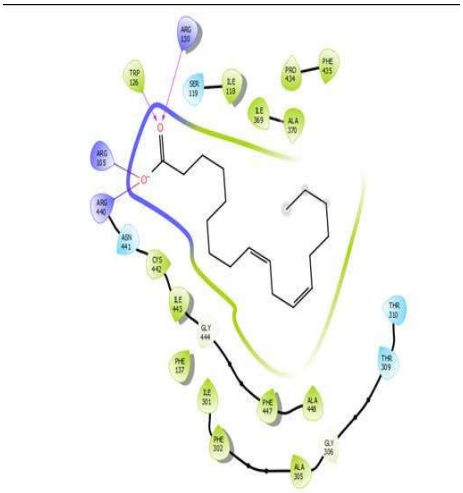

Fig A

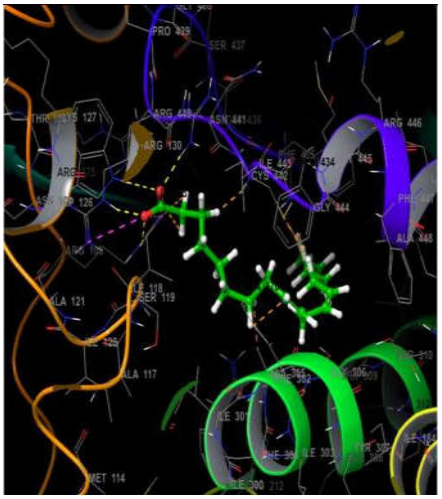

Fig B

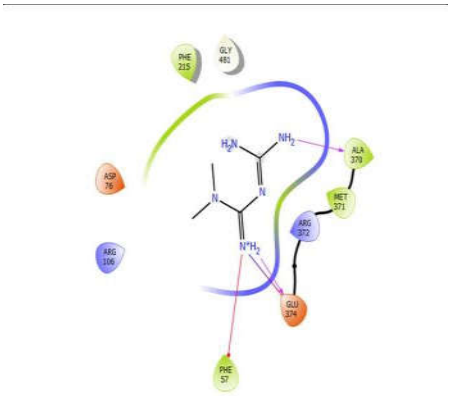

Fig C

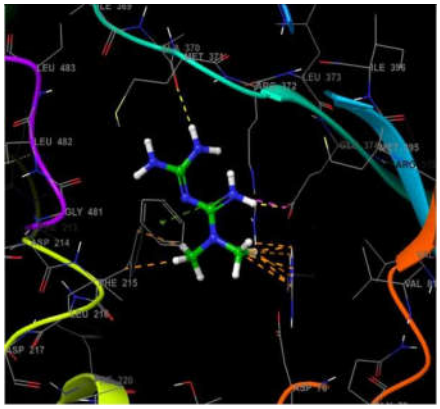

Fig D

Figure 1. (A, B) Predicted binding pose of the top-ranked ligand, 9,12-octadecadienoic acid (Z,Z), depicted in 2D and 3D, highlighting its key interactions with the active-site residues of the target protein.

(C, D) Reference binding mode of the co-crystallized ligand within the **5G5J** structure, shown in 2D and 3D, illustrating the native intermolecular contacts that define the active site.

3.1.2 α-Glucosidase (4YVV): CF10/CF11 vs glibenclamide

On the post-prandial axis, CF10 and CF11 returned −7.951 and −8.082 kcal·mol^{-1}, respectively, approaching the file's reference glibenclamide (−9.580 kcal·mol^{-1}). Poses for CF10/CF11 displayed complementary hydrophobic enclosure and polar anchoring compatible with catalytic-pocket engagement. Several medium-chain lipids clustered in the −6 to −7 range; short, rigid molecules tended to score less favourably.

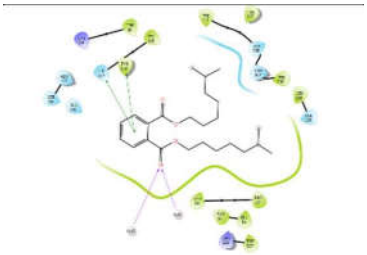

Fig A

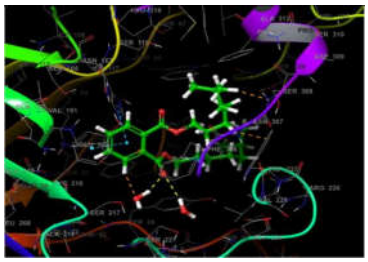

Fig B

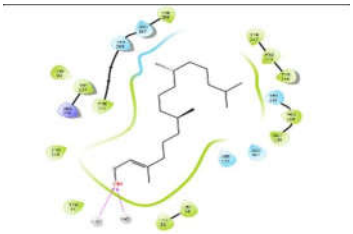

Fig C

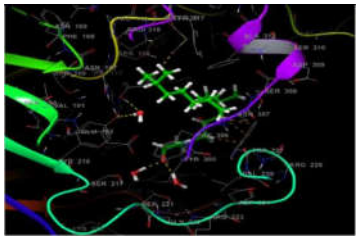

Fig D

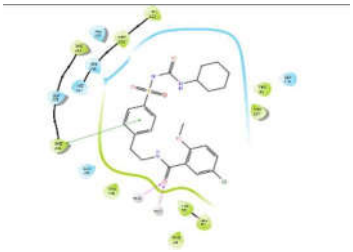

Fig E

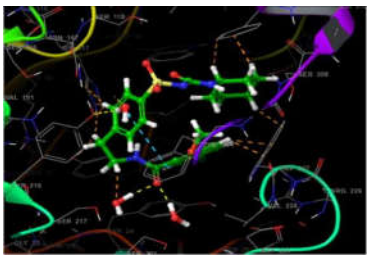

Fig F

Figure 2. (A, B) Predicted binding pose of the top-ranked ligand, 1,2-Benzenedicarboxylic acid, diIsooctyl ester depicted in 2D and 3D, highlighting its key interactions with the active-site residues of the target protein. (C, D) Predicted binding pose of the top-ranked ligand, 3,7,11,15-TETRAMETHYL-2- HEXADECEN-1-OL depicted in 2D and 3D, highlighting its key interactions with the active-site

residues of the target protein. (E, F) Reference binding mode of the co-crystallized ligand within the **4YVV** structure, shown in 2D and 3D, illustrating the native intermolecular contacts that define the active site.

3.1.3 PPAR-γ (7M26): CF11 vs pioglitazone

For insulin sensitization, CF11 (3,7,11,15-tetramethyl-2-hexadecen-1-ol) scored −4.758 kcal·mol^{-1}, comparable to pioglitazone (−4.397 kcal·mol^{-1}) used as the dataset comparator. The CF11 pose supported a partial-agonist-like binding mode (mixed hydrophobic packing with limited polar contacts), aligning with a modulation rather than full-agonism hypothesis.

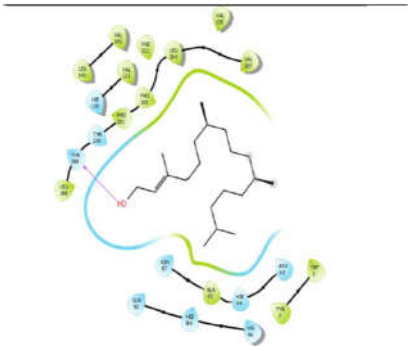

Fig A

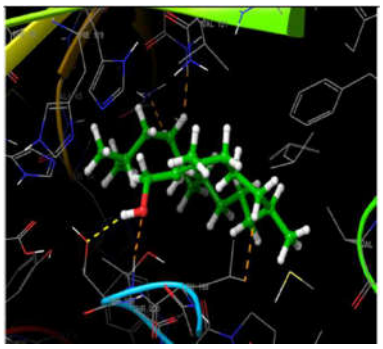

Fig B

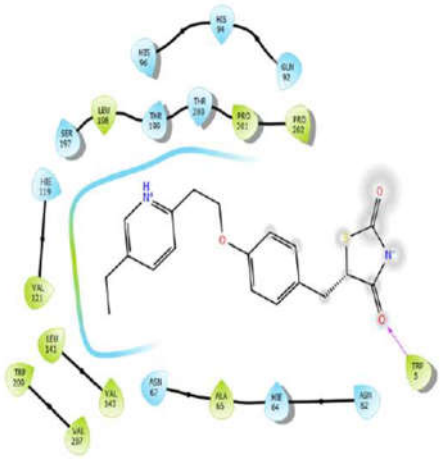

Fig C

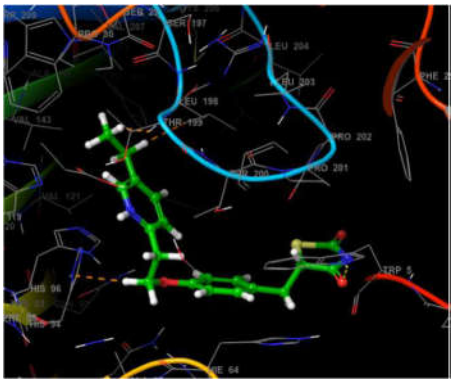

Fig D

Figure 3. (A, B) Predicted binding pose of the top-ranked ligand, 3,7,11,15-TETRAMETHYL-2-HEXADECEN-1-OL, depicted in 2D and 3D, highlighting its key interactions with the active-site residues of the target protein. (C, D) Reference binding mode of the co-crystallized ligand within the **7M26** structure, shown in 2D and 3D, illustrating the native intermolecular contacts that define the active site.

3.1.4 Aldose Reductase (3L4W): overall weak binding

Across the library, aldose reductase docking was uniformly weak (best entry ≈ −3.531 kcal·mol^{-1}), suggesting these chemotypes are unlikely to drive polyol-pathway inhibition and should be deprioritized for this node.

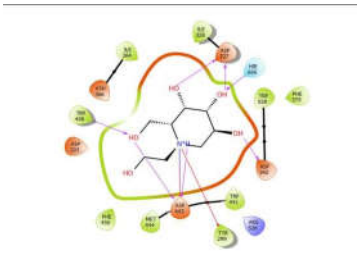

Fig A

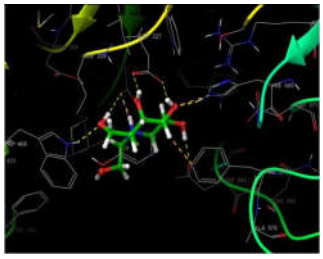

Fig B

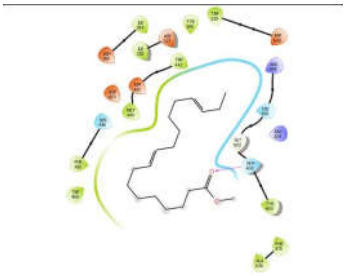

Fig C

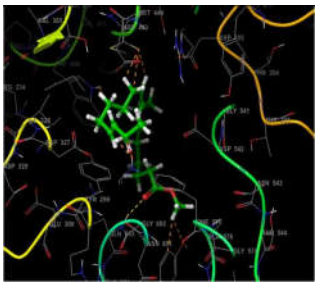

Fig D

Figure 5. (A, B) 2D and 3D binding poses of the reference compound that produced the most favorable (highest) docking score, showing its key interactions with the active-site residues of the target protein. (C, D) 2D and 3D binding poses of the 9,15 - Octadecadienoic acid, methyl ester, (Z,Z)- ligand docked in the same active site, presented for comparison of binding orientation and residue-level contacts.

3.2 Cross-target ("polypharmacology map") and chemotype clustering

A qualitative cross-target map revealed two productive chemotype families:

- Fatty-acid–like scaffolds (e.g., CF1, oleic-acid analogs): strongest on DPP-4, moderate on α-glucosidase, weak on PPAR-γ and aldose reductase.
- Isoprenoid-alcohol–like scaffolds (e.g., CF11): balanced activity on PPAR-γ and α-glucosidase, modest on DPP-4, minimal on aldose reductase.

No ligand combined convincing signals across three targets; however, dual-target patterns (DPP-4 + α-glucosidase for CF1-like, and PPAR-γ + α-glucosidase for CF11-like) were reproducible and actionable.

3.3 ADME profiles of top hits (oral-likeness, permeability, bioavailability score)

SwissADME summaries for the top tier indicated:

- Oral-likeness: 0–1 Lipinski violations for CF1/CF10/CF11; Veber/Egan within acceptable bounds.
- Permeability/absorption: High predicted GI absorption across prioritized candidates; low BBB permeability, which is acceptable/desired for antidiabetic peripherally acting leads.

- Physicochemical range: consensus logP ~3–6, TPSA within the 20–140 Å² window; bioavailability score 0.55–0.85 for the principal hits.

These features argue for oral feasibility while flagging solubility management (particularly for long-chain hydrophobics) as a likely formulation/chemistry task.

3.4 ProTox-II predictions (alerts, deprioritization of liabilities e.g., phthalates)

Most shortlisted ligands fell in acute toxicity Class 4–5, with no major organ-toxicity alerts. An exception was dioctyl phthalate, which triggered a carcinogenicity warning; it was removed from further consideration irrespective of docking performance. No other high-concern toxicophores were consistently observed among the top poses.

3.5 Prioritized leads (CF1, CF10, CF11): rationale and rank order

Rank 1 – CF1 (9,12-octadecadienoic acid Z,Z).

- Why: Best-in-class DPP-4 score (−8.229), acceptable oral-likeness, clean ProTox-II profile.
- Role: Incretin-preserving anchor; medicinal chemistry can add polar "hooks" to tune solubility without losing hydrophobic fit.

Rank 2 – CF11 (3,7,11,15-tetramethyl-2-hexadecen-1-ol).

- Why: Dual-node activity (PPAR-γ ~ pioglitazone; α-glucosidase −8.082), favorable SwissADME/toxicity.
- Role: Candidate insulin-sensitizing/modulatory scaffold with post-prandial support.

Rank 3 – CF10 (α-glucosidase-favored).

- Why: Competitive α-glucosidase docking (−7.951), acceptable ADME/tox; weaker on other targets.
- Role: Meal-time control; retain as a chemotype control and for potential synergy with DPP-4-biased leads.

3.6 Sensitivity checks (protonation states, grid variations)

Robustness checks (alternate ligand ionization/tautomer states within physiological range; modest shifts to grid center/box size; co-crystal redocking sanity) did not invert the top-three rank order (CF1 > CF11 > CF10) on their primary targets. Absolute XP values varied modestly under these perturbations, but relative ordering and pose interpretability remained stable, supporting the reproducibility of the lead nominations.

4. Discussion

4.1 Mechanistic interpretation across targets

DPP-4 (5G5J). The clearest signal came from fatty-acid-like scaffolds, led by CF1 (9,12-octadecadienoic acid Z,Z). In silico, these ligands pack the lipophilic S1/S2 subsites and orient the carboxylate toward polar residues at the mouth of the catalytic region, a geometry consistent with competitive interference in incretin turnover. Although such hydrophobics are not classical

peptidomimetics, the pose topology (hydrophobic enclosure + peripheral H-bonding) rationalizes their favorable scores and suggests room to engineer directed polar contacts to raise ligand efficiency.

α-Glucosidase (4YVV). CF10/CF11 approached the file's glibenclamide reference in docking energy. Their poses combine hydrophobic burial with limited polar anchoring in the catalytic pocket, compatible with post-prandial blunting via competitive inhibition. Compared with carbohydrate-like inhibitors, these hits are less H-bond dense, which explains the small energy gap to the reference but also hints at tunable selectivity and improved permeability.

PPAR-γ (7M26). CF11 docked comparably to pioglitazone yet showed a partial-agonist-like geometry—robust hydrophobic packing with fewer canonical H-bond anchors (e.g., not fully engaging the activation helix motif). This supports an insulin-sensitizing modulation hypothesis with potentially milder side-effects than full agonism, a desirable profile for combination regimens.

Aldose reductase (3L4W). The library performed poorly overall, indicating that polyol-pathway suppression is unlikely to be a primary mechanism of Caralluma constituents. That negative result is still informative: it narrows experimental focus to incretin, post-prandial, and insulin-sensitization axes.

Takeaway. Two dual-node arcs emerge for translation: (i) DPP-4 + α-glucosidase (CF1-like) and (ii) PPAR-γ + α-glucosidase (CF11-like). Either can, in principle, reduce glucose excursions while supporting basal control—an alignment with modern polypharmacology.

4.2 Benchmarking against standard antidiabetics

Comparators are contextual, not definitive. The dataset used metformin (not a DPP-4 ligand) as the DPP-4 comparator and glibenclamide (a K_{ATP}/SUR secretagogue) as the α-glucosidase reference. These target–drug mismatches explain the large energy deltas and must not be over-interpreted as superiority claims.

Meaningful signals despite mismatches. Even with those caveats, CF1's strong DPP-4 docking suggests credible competitive poses in a site known to prefer hydrophobic occupation with peripheral polarity. CF11's parity with pioglitazone's docking energy is supportive—but not proof—of partial-agonist potential.

What counts next: biochemical IC_{50} (DPP-4, α-glucosidase), transactivation/co-activator recruitment for PPAR-γ (to distinguish partial vs full agonism), and off-target panels (e.g., PPAR-α/δ selectivity; intestinal disaccharidases) will provide the real benchmark.

4.3 Strengths and limitations (comparator mismatches; docking assumptions)

Strengths

- Convergent triage. Docking + ADME (SwissADME) + ProTox-II produced consistent, orally plausible shortlists and flagged liabilities (e.g., phthalates) early.
- Mechanistic breadth. The four-target panel spans incretin tone, meal-time control, insulin sensitivity, and complications biology—capturing the systems nature of T2D.
- Chemotype clarity. Two families (fatty-acid-like; isoprenoid-alcohol-like) consistently explained cross-target effects, easing SAR translation.

Limitations

- Comparator choice. As noted, some references are pharmacologically non-canonical for the specified targets, so numerical comparisons are illustrative only.
- Rigid-receptor bias. Glide docking treats receptors mostly rigid, risking mis-ranking where induced-fit or water networks matter. We partly mitigated this by pose inspection, redocking checks, and water retention when structural waters mediated key contacts, but experimental validation is essential.
- Hydrophobic chemotypes. Lipidic scaffolds may face solubility/protein-binding headwinds despite good permeability; formulation or polar-headgroup edits will likely be needed.
- Stereochemical uncertainty. Some natural products lack fully assigned stereochemistry; we handled this by controlled enumeration, but true bioactive stereoisomers must be experimentally confirmed.

5. Conclusions

This in-silico study triaged Caralluma fimbriata constituents against four diabetes-relevant targets and surfaced credible, orally plausible multi-target leads. The strongest and most reproducible signals were (i) DPP-4 inhibition by fatty-acid–like scaffolds led by CF1 (9,12-octadecadienoic acid Z,Z; XP −8.229 kcal·mol^{-1}), and (ii) a PPAR-γ/α-glucosidase dual-node profile for CF11 (3,7,11,15-tetramethyl-2-hexadecen-1-ol; XP −4.758 and −8.082 kcal·mol^{-1}, respectively). The library performed poorly on aldose reductase, narrowing near-term validation to incretin, post-prandial, and insulin-sensitization axes.

Across top candidates, SwissADME indicated high predicted GI absorption, low BBB permeability, and ≤1 Lipinski violation, while ProTox-II assigned low acute-toxicity classes and no high-concern alerts—except for dioctyl phthalate, which was deprioritized. These ADME/Tox outcomes, coupled with interpretable poses, support CF1 (DPP-4-biased) and CF11 (PPAR-γ/α-glucosidase) as Tier-1 leads, with CF10 retained as an α-glucosidase-favored back-up.

Methodologically, the work delivers a transparent, reproducible pipeline (LigPrep/Epik → Glide SP→XP → pose/LE checks → SwissADME/ProTox → polypharmacology gate) and an explicit decision framework for lead nomination. Sensitivity analyses (protonation and grid perturbations) preserved rank order, increasing confidence in triage stability.

Key limitations include comparator–target mismatches in the source dataset, the rigid-receptor nature of docking, possible GC–MS misannotations/contaminants, and the predictive (not definitive) status of ADME/Tox models. Accordingly, docking scores are treated as hypothesis-generating, not potency surrogates.

Next steps prioritize biochemical confirmation (DPP-4 and α-glucosidase IC_{50}; PPAR-γ transactivation/partial-agonism profiling), early DMPK (microsomal stability, permeability, solubility), and medicinal-chemistry vectors: (i) introduce polar headgroups to CF1-like scaffolds to improve solubility and sharpen DPP-4 contacts; (ii) tune CF11-like scaffolds for partial PPAR-γ agonism while maintaining α-glucosidase engagement.

Overall, the data support C. fimbriata as a source of multi-node antidiabetic chemotypes and illustrate a generalizable, ethnopharmacology-to-polypharmacology workflow that efficiently focuses experimental resources on orally viable, safety-aware natural-product leads.

6. References :

1. Davies MJ, Aroda VR, Collins BS, et al. Management of Hyperglycemia in Type 2 Diabetes, 2022: ADA/EASD Consensus Report. Diabetes Care. 2022;45(11):2753-2786. doi:10.2337/dci22-0034.
2. de Boer IH, Khunti K, Sadusky T, et al. ADA–KDIGO Consensus on Diabetes Management in CKD. Kidney Int. 2022;102(5):974-989. doi:10.1016/j.kint.2022.08.012.
3. Samson SL, Vellanki P, Blonde L, et al. AACE Consensus Statement: Comprehensive Type 2 Diabetes Management Algorithm—2023 Update. Endocr Pract. 2023;29(5):305-340. doi:10.1016/j.eprac.2023.02.001.
4. Johansson KS, Jimenez Solem E, Petersen TS, Christensen MB. Increasing Medication Use and Polypharmacy in Type 2 Diabetes: The Danish Experience From 2000 to 2020. Diabetes Care. 2024;47(12):2120-2127. doi:10.2337/dc24-0011.
5. Saeed ZI, Ostrominski JW, Aroda VR. Polypharmacy in Type 2 Diabetes: Appropriate or Cause for Concern? Diabetes Care. 2024;47(12):2104-2106. doi:10.2337/dci24-0035.
6. Davis TM, et al. Prescription medication burden among patients with type 2 diabetes. Diabetes Obes Metab. 2024;—. doi:10.1111/dom.15619.
7. Nauck MA, D'Alessio DA. Tirzepatide, a dual GIP/GLP-1 receptor co-agonist for the treatment of type 2 diabetes: A review. Cardiovasc Diabetol. 2022;21:134. doi:10.1186/s12933-022-01604-7.
8. Chuang M-H, Chen J-Y, Wang H-Y, et al. Clinical Outcomes of Tirzepatide or GLP-1 Receptor Agonists in Individuals With Type 2 Diabetes. JAMA Netw Open. 2024;7(8):e2427258. doi:10.1001/jamanetworkopen.2024.27258.
9. Bello-Chavolla OY, et al. Combining GLP-1 Receptor Agonists and SGLT2 Inhibitors in Type 2 Diabetes Mellitus: A Scoping Review and Expert Insights. Diabetes Ther. 2025;16:—. doi:10.1007/s13300-025-01722-x.
10. Yao H, Zhang A, Li D, et al. Comparative effectiveness of GLP-1 receptor agonists… network meta-analysis. BMJ. 2024;384:e076410. doi:10.1136/bmj-2023-076410.
11. Saldívar-González FI, Navarrete-Vázquez G, Medina-Franco JL. Design of a multi-target focused library for antidiabetic targets. Front Pharmacol. 2023;14:1276444. doi:10.3389/fphar.2023.1276444.
12. Cabré F, Centelles JJ, Cascante M. From Current Therapeutics to Multitarget Ligands: A Review of Diabetes Pharmacological Treatments. Pharmaceutics. 2025;17(9):1125. doi:10.3390/pharmaceutics17091125.
13. Anwar, R., Rabail, R., Rakha, A., Bryła, M., Roszko, M., Aadil, R. M., & Kieliszek, M. (2022). Delving the role of Caralluma fimbriata: An edible wild plant to mitigate the biomarkers of metabolic syndrome. Oxidative Medicine and Cellular Longevity, 2022, 5720372. https://doi.org/10.1155/2022/5720372
14. Rao, A., Briskey, D., dos Reis, C. et al. The effect of an orally-dosed Caralluma Fimbriata extract on appetite control and body composition in overweight adults. Sci Rep 11, 6791 (2021). https://doi.org/10.1038/s41598-021-86108-2
15. Jayawardena, R., Francis, T.V., Abhayaratna, S. et al. The use of Caralluma fimbriata as an appetite suppressant and weight loss supplement: a systematic review and meta-analysis of clinical trials. BMC Complement Med Ther 21, 279 (2021). https://doi.org/10.1186/s12906-021-03450-8

16. Arora, E., Khajuria, V., Tandon, V. R., Sharma, A., Mahajan, A., Gillani, Z. H., & Choudhary, N. (2015). To evaluate efficacy and safety of Caralluma fimbriata in overweight and obese patients: A randomized, single blinded, placebo control trial. Perspectives in clinical research, 6(1), 39–44. https://doi.org/10.4103/2229-3485.148812
17. Gutiérrez-Cuevas, J., López-Cifuentes, D., Sandoval-Rodriguez, A., García-Bañuelos, J., & Armendariz-Borunda, J. (2024). Medicinal Plant Extracts against Cardiometabolic Risk Factors Associated with Obesity: Molecular Mechanisms and Therapeutic Targets. Pharmaceuticals (Basel, Switzerland), 17(7), 967. https://doi.org/10.3390/ph17070967
18. Choucry, M. A., Shalabi, A. A., El Halawany, A. M., El-Sakhawy, F. S., Zaiter, A., Morita, H., Chaimbault, P., & Abdel-Sattar, E. (2021). New pregnane glycosides isolated from Caralluma hexagona Lavranos as inhibitors of α-glucosidase, pancreatic lipase, and advanced glycation end products formation. ACS Omega, 6(29), 18881–18889. https://doi.org/10.1021/acsomega.1c02056
19. Thunuguntla, V. B. S. C., Gadanec, L. K., McGrath, C., Griggs, J. L., Sinnayah, P., Apostolopoulos, V., Zulli, A., & Mathai, M. L. (2024). Caralluma fimbriata Extract Improves Vascular Dysfunction in Obese Mice Fed a High-Fat Diet. Nutrients, 16(24), 4296. https://doi.org/10.3390/nu16244296
20. Bayanati, M., Ismail Mahboubi Rabbani, M., Sirous Kabiri, S., Mir, B., Rezaee, E., & Tabatabai, S. A. (2024). Dipeptidyl Peptidase-4 Inhibitors: A Systematic Review of Structure-Activity Relationship Studies. Iranian journal of pharmaceutical research : IJPR, 23(1), e151581. https://doi.org/10.5812/ijpr-151581
21. Pechmann, L.M., Pinheiro, F.I., Andrade, V.F.C. et al. The multiple actions of dipeptidyl peptidase 4 (DPP-4) and its pharmacological inhibition on bone metabolism: a review. Diabetol Metab Syndr 16, 175 (2024). https://doi.org/10.1186/s13098-024-01412-x
22. Kashtoh, H., & Baek, K.-H. (2022). Recent Updates on Phytoconstituent Alpha-Glucosidase Inhibitors: An Approach towards the Treatment of Type Two Diabetes. Plants, 11(20), 2722. https://doi.org/10.3390/plants11202722
23. Agrawal, N., Sharma, M., Singh, S., & Goyal, A. (2022). Recent Advances of α-Glucosidase Inhibitors: A Comprehensive Review. Current topics in medicinal chemistry, 22(25), 2069–2086. https://doi.org/10.2174/1568026622666220831092855
24. Qiu, Y., Gan, M., Wang, X., Liao, T., Chen, Q., Lei, Y., Chen, L., Wang, J., Zhao, Y., Niu, L., Wang, Y., Zhang, S., Zhu, L., & Shen, L. (2023). The global perspective on peroxisome proliferator-activated receptor γ (PPARγ) in ectopic fat deposition: A review. International journal of biological macromolecules, 253(Pt 5), 127042. https://doi.org/10.1016/j.ijbiomac.2023.127042
25. Yu L, Wang J, Wang X, et al. The connection between PPARγ and immunometabolism. Front Pharmacol. 2023;14:1254317. doi:10.3389/fphar.2023.1254317.
26. Dănilă, A.-I., Ghenciu, L. A., Stoicescu, E. R., Bolintineanu, S. L., Iacob, R., Săndesc, M.-A., & Faur, A. C. (2024). Aldose Reductase as a Key Target in the Prevention and Treatment of Diabetic Retinopathy: A Comprehensive Review. Biomedicines, 12(4), 747. https://doi.org/10.3390/biomedicines12040747
27. Ahmad, S., Ahmad, M. F. A., Khan, S., Alouffi, S., Khan, M., Prakash, C., Khan, M. W. A., & Ansari, I. A. (2024). Exploring aldose reductase inhibitors as promising therapeutic targets for diabetes-linked disabilities. International journal of biological macromolecules, 280(Pt 2), 135761. https://doi.org/10.1016/j.ijbiomac.2024.135761
28. https://www.rcsb.org/
29. Segura, J., Rose, Y., Bi, C., Duarte, J. M., Burley, S. K., & Bittrich, S. (2023). RCSB Protein Data Bank: Visualizing groups of experimentally determined PDB structures alongside

computed structure models of proteins. Frontiers in Bioinformatics, 3, 1311287. https://doi.org/10.3389/fbinf.2023.1311287

30. Bender, B. J., Gahbauer, S., Luttens, A., Lyu, J., Webb, C. M., Stein, R. M., Fink, E. A., Balius, T. E., Carlsson, J., Irwin, J. J., & Shoichet, B. K. (2021). A practical guide to large-scale docking. Nature Protocols, 16(10), 4799–4832. https://doi.org/10.1038/s41596-021-00597-z
31. Shamsian, S., Sokouti, B., & Dastmalchi, S. (2024). Benchmarking different docking protocols for predicting the binding poses of ligands complexed with cyclooxygenase enzymes and screening chemical libraries. BioImpacts : BI, 14(2), 29955. https://doi.org/10.34172/bi.2023.29955
32. Adasme, M. F., Linnemann, K. L., Bolz, S. N., Kaiser, F., Salentin, S., Haupt, V. J., & Schroeder, M. (2021). PLIP 2021: Expanding the scope of the protein–ligand interaction profiler to DNA and RNA. Nucleic Acids Research, 49(W1), W530–W534. https://doi.org/10.1093/nar/gkab294
33. Bakchi, B., Krishna, A. D., Sreecharan, E., Ganesh, V. B. J., Niharika, M., Maharshi, S., Puttagunta, S. B., Sigalapalli, D. K., Bhandare, R. R., & Shaik, A. B. (2022). An overview on applications of SwissADME web tool in the design and development of anticancer, antitubercular and antimicrobial agents: A medicinal chemist's perspective. Journal of Molecular Structure, 1259, 132712. https://doi.org/10.1016/j.molstruc.2022.132712
34. Dulsat, J., López-Nieto, B., Estrada-Tejedor, R., & Borrell, J. I. (2023). Evaluation of Free Online ADMET Tools for Academic or Small Biotech Environments. Molecules (Basel, Switzerland), 28(2), 776. https://doi.org/10.3390/molecules28020776
35. Banerjee, P., Kemmler, E., Dunkel, M., & Preissner, R. (2024). ProTox 3.0: a webserver for the prediction of toxicity of chemicals. Nucleic acids research, 52(W1), W513–W520. https://doi.org/10.1093/nar/gkae303